Study of the Visual Evoked Magnetic Field with the M-Sequence Technique

Hitoshi Tabuchi,[1] Tsuranu Yokoyama,[2] Masahiro Shimogawara,[3] Kunihiko Shiraki,[1] Eiichiro Nagasaka,[4] and Tokuhiko Miki[1]

PURPOSE. Multifocally stimulated visual evoked magnetic field (VEF) examination with an m-sequence technique (multifocal VEF; mVEF) was studied, and the neural generators at peaks of mVEF were estimated in the visual cortex.

METHODS. Visual field stimulation was generated by a multifocal testing system with use of the m-sequence technique. The stimulation pattern covered a central area extending from 0.6° to 10° in radius outward from the center of four visual-field quadrants. The stimulation pattern was projected onto a screen by a liquid crystal projector. VEFs of 14 healthy adults were recorded with a 160-channel, whole-head-type magnetoencephalography (MEG) system. The output signals of 16 selected MEG sensors covering the occipital region were recorded for each subject with the multifocal testing system, and the second-order responses were calculated. The analyzed response data files were transferred to the MEG system, a single equivalent current dipole (ECD) was estimated to locate the neural generator, and the localization was superimposed onto the corresponding brain magnetic resonance image of the subject.

RESULTS. mVEFs showed three peak waves (N75m, P100m, N145m) in 75% of the subjects and two peak waves (N75m, N145m) in 25%. (N, P and m denote negative, positive, and magnetic fields, respectively.) Latencies of the first and the last peak were similar between the two kinds of peak waves. ECD examination showed more than 97% of goodness of fit at all peaks, and the relation between EDCs and the stimulated visual field coincided with a retinotopic organization that fit a cruciform model in all subjects. ECD depths from the occipital pole were similar to the depth expected from the human linear cortical magnification factor model in all subjects. Main neural generators of all mVEF components (N75m, P100m, N145m) were shown in the striate cortex (V1).

CONCLUSIONS. Testing the VEF with an m-sequence technique showed stable responses to simultaneous stimulation of four visual-field quadrants. Consistency of correlation of the estimated ECD with the known cortical organization of the primary visual cortex confirmed the reliability of this examination. The three mVEF peaks were thought to derive mainly from V1 activity. (*Invest Ophthalmol Vis Sci.* 2002;43:2045–2054)

Magnetoencephalography (MEG) and electroencephalography (EEG) examine the activity of identical neurons in a different way.[1,2] Conduction of multiple signals distorts EEG measurement within the head, whereas MEG is essentially unaffected by electrical complexity.[3] Thus, MEG estimates the equivalent current dipole (ECD), which is a source of brain activity, more accurately than EEG does. The high spatiotemporal resolution of MEG enables researchers to anatomically localize ECDs in the human visual cortex, by using the visual evoked magnetic field (VEF).[4-9] The VEF consists of three main components, N75m, P100m, and N145m, and studies of visual evoked potential (VEP) and VEF have shown differences in the physiologic characters of three components.[10-13] (N, P and m denote negative, positive, and magnetic fields, respectively.) In previous studies of ECDs of VEF components, both Nakamura et al.[8] and Shigeto et al.[6] reported that the N75m and P100m components were generated in the striate cortex, but Nakamura et al. reported that the N145m component was generated in the extrastriate cortex, and Shigeto et al. reported that it was generated in the striate cortex. Similar differences in ECD locations were reported previously in relation to VEP components.[14-19]

The discrepant findings may be due to the different methods of signal stimulation or to the structural complexity of the visual cortex. Functional retinotopy of the human visual cortex is well known to fit a cruciform model.[20-23] Right and left visual fields project into the opposite hemisphere of the primary visual cortex. The upper field projects into the cortex below the calcarine sulcus, whereas the lower field projects into the cortex above the sulcus. Thus, with a full-field stimulus, magnetic fields generated by the four regions of the visual cortex cancel each other, and the obtained results do not precisely reflect the response of the cortical regions. Nakamura et al.[8] stimulated the temporal or nasal half of the visual field, but this stimulation was still too large to avoid cancellation between the upper and lower areas of the visual fields. To avoid this type of signal cancellation, the stimulus size must be no greater than or equal to one quadrant. Too small a stimulus, however, would lose the signal-to-noise ratio of the response during a short stimulation time. For instance, a stable response was not acquired with stimulation of a quadrant of visual fields in the report of Shigeto et al.[6] In addition to the size of each stimulus, a decrease in a subject's mental concentration on fixation limits the number of locations in sequential visual field stimulation.

These general problems can be overcome with the m-sequence technique of pseudorandomly presented multifocal stimulation,[24] and this technique has been applied to recording of VEPs—namely, multifocal VEPs (mVEPs). In previous studies of mVEPs, the m-sequence technique showed individual responses at each of multiple stimulated locations.[25-33] Even with the m-sequence technique, ECD estimation with VEP has some errors. Because the structure of the visual cortex is complex, the direction of the vector of each response would be diverse at the visual cortex. Furthermore, interindividual anatomic variation of the visual cortex is considerable. There-

fore, many optimum sensors are necessary to pick up the responses of the various directions on the scalp. MEG can record many channels simultaneously, because it does not require placement of sensors. VEF combined with the m-sequence technique is therefore a method that should be tested for examination of the responses from multifocal stimulation and for precise estimation of a source of the visual cortex activity. Slotnick et al.[26] obtained ECDs by using the multichannel mVEP; however, they examined only the one mVEP component with the highest reliability of three components and confirmed that the relative relationship of ECDs fit to the cruciform model, without clarifying the anatomic relation of the ECDs with the calcarine sulcus, which is an important landmark in the cruciform model.

In our present study, we first examined the reliability of the mVEF by studying whether the anatomic distribution of acquired ECDs to the longitudinal fissure and the calcarine sulcus confirm to the cruciform model and whether the depth of the ECDs from the occipital pole fit the theory of a human linear cortical magnification factor.[21] We then studied the source localization of each peak component of mVEFs in the visual cortex.

METHODS

Subjects

Fourteen healthy volunteers (12 men and 2 women, aged 24–40 years) were recruited to participate in the study. All of them had corrected visual acuity of 20/20 or better, and none had a history of ophthalmic or neural abnormality. The right eye was examined, and the left eye was covered with an eye bandage during the recording. Experiments were conducted in accordance with principles embodied in the Declaration of Helsinki. All subjects were fully informed of the nature, purpose, and minimal risks of these experiments, and consent was obtained from each individual.

Stimulus

The multistimulus array shown in Figure 1 consists of four quadrants, each extending 0.6° to 10° out along the radius of the visual field. According to the human linear cortical magnification factor, the stimulus area was chosen to avoid activating the visual cortex area wrapping around the occipital pole and extending into the lateral convexity. Each checkerboard quadrant was simultaneously modulated with a shifted binary m-sequence[24,25] by a visual evoked response imaging system (VERIS; VERIS Science, EDI Corp., San Mateo, CA). The length of the m-sequence was $2^{13} - 1$, corresponding to 8191 stimulus frames. Therefore, 4096 pattern-reversal stimuli were delivered in the sequence for each quadrant. The recording session was broken up into eight 34-second data-collection segments. As a result, it took 4 minutes 32 seconds to complete one examination. The stimulus image was projected onto a screen with a liquid crystal display (LCD) projector (VPL200EX; Sony, Tokyo, Japan) that has a delay time of 20 ± 1.0 ms. Although the vertical scanning rate of the LCD projector we used is 60 Hz, the stimulus rate was reduced to 30 Hz with two consecutive stimulus frames to avoid overlapping stimulation caused by the delay of the LCD projector. The screen was placed 27 cm in front of the right eye. The luminance of the checkerboard's white and in black checks was 72 and 7 cd/m^2, respectively. Thus, the contrast (the difference between luminance of the white and black checks, divided by their sum) was 82%.

Magnetoencephalography

All MEG sessions were conducted in a magnetically shielded room at Osaka City University Hospital with the use of a whole-head type, 160-channel MEG system (PQ1160C; Yokogawa Electric Corp., Tokyo,
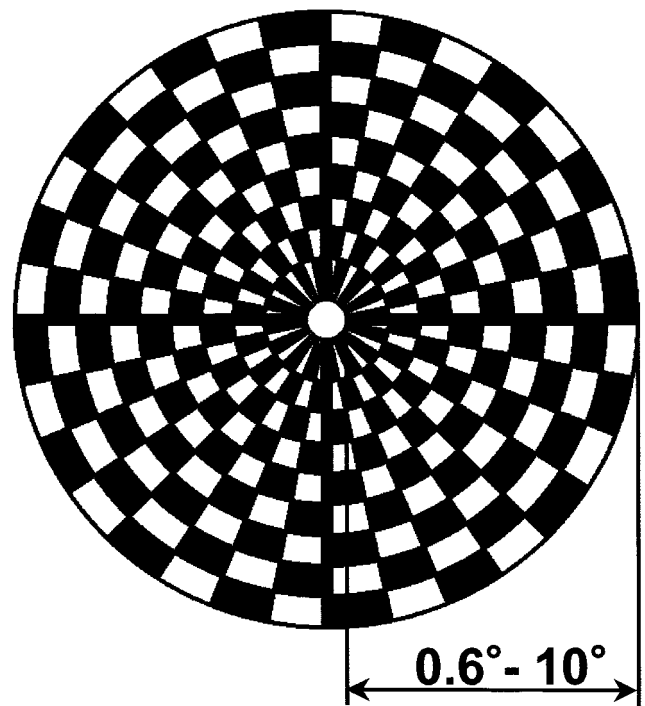

FIGURE 1. Multistimulus array used to stimulate four quadrants designated from 0.6° to 10° away from the center of the visual field. The stimulus range was chosen to avoid activating the visual cortex area close to the occipital pole and extending onto the lateral convexity. Each quadrant consists of nine (in radial) × eight (in arc) checks and reverses, synchronized with the binary m-sequence allocated in each part.

Japan). The pick-up coils were on a first-order gradiometer with a 50-mm baseline and a 15.5-mm diameter. The experiments were conducted with the subjects supine, which is relaxing and prevents motion artifacts.[34] The output signals of 16 selected MEG sensors covering the occipital region were recorded with the VEP imaging system. Signals were amplified 10,000 times, passed through a 3- to 100-Hz band-pass filter and digitized at a sampling rate of 1000 Hz. To confirm reproducibility, the recording was obtained twice in all subjects. Second-order responses were calculated by the visual evoked response system with the use of a cross-correlation method.[24] Four 16-channel responses corresponding to each quadrant of the visual field were obtained at every measurement. Analyzed wave data files were transferred to the MEG system and corrected for the delay time of the LCD projector.

Dipole Estimate on Magnetic Resonance Images at Peaks of All mVEFs

A single ECD model in spherical volume conduction[35] was used to estimate neural source at all peaks of mVEF. All subjects were also scanned with a magnetic resonance (MR) imaging system with 1.5- to 5.0-mm slice thickness. ECDs, which were estimated from all mVEF-peaks of all subjects, were superimposed on the MR images to examine whether the relation between the stimulated visual field and the acquired ECDs fit the cruciform model and human linear cortical magnification factor. As an indicator of the quality of estimation, goodness of fit (GOF)[36] was also calculated.

Comparison of mVEF-Estimated ECDs with Theoretical ECDs

By combined use of the human linear cortical magnification factor and the cruciform model, the anatomic location of an ECD can be defined
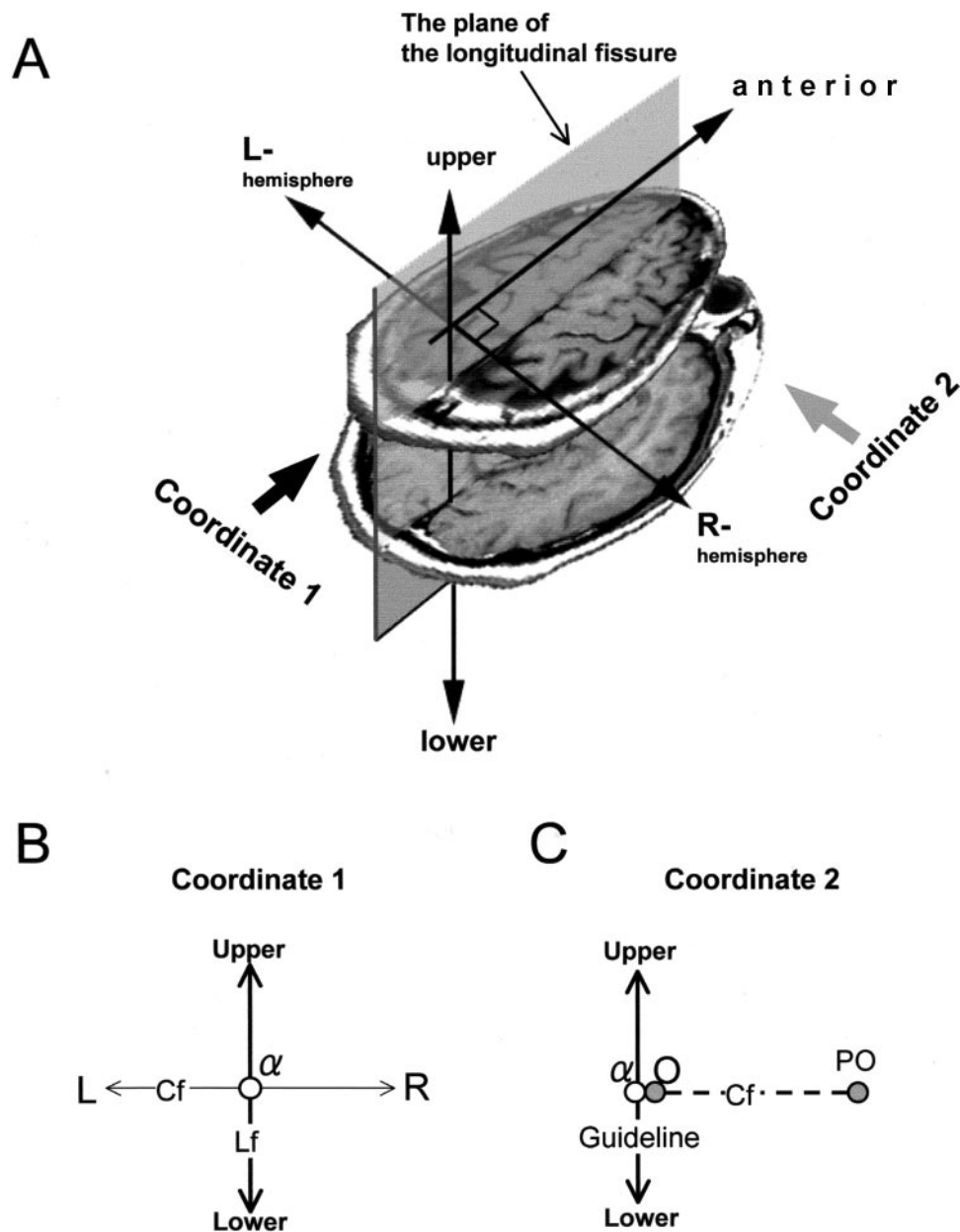
FIGURE 2. Coordinates for the evaluation of anatomic locations of ECDs. (**A**) Three-dimensional relation between the coordinate planes 1 and 2. (**B**) In the plane of coordinate 1, the abscissa is the left–right axis, showing the distance from the longitudinal fissure (Lf), and the ordinate is the upper–lower axis, showing height from the calcarine sulcus (Cf). The crossing point (α) is defined as the position of an ECD on the calcarine sulcus. (**C**) In the plane of coordinate 2, the abscissa is the anterior–posterior axis, showing the depth of ECDs from the occipital pole along the calcarine sulcus, and the ordinate is the upper–lower axis. The ECD height is shown as a percentage ratio of the distance from the calcarine sulcus, and the depth is the ratio from the occipital pole to the total length of the calcarine sulcus, that is from the occipital (O) pole to the parieto-occipital (PO) sulcus.

in three-dimensional space of the visual cortex (Fig. 2A). The position of an ECD was determined by measuring distance from the longitudinal fissure plane, height from the calcarine sulcus plane, and depth along the calcarine sulcus from the occipital pole. Thus, mVEF-produced ECDs were plotted on two coordinate planes. The first coordinate plane corresponds to a coronal section of an MR image. The abscissa shows distance of an ECD from the longitudinal fissure plane, and this axis is designated as the left-to-right axis. The ordinate shows height of an ECD from the calcarine sulcus plane, and this axis is designated as the upper-to-lower axis (Fig. 2B). Because the calcarine sulcus plane is

a curvilinear, the height from the calcarine sulcus was defined in the following way (Fig. 3): Because retinotopy theory maintains that areas at the same eccentricity in the visual field project to regions symmetrical to the calcarine sulcus in the visual cortex,[20,21] two ECDs were produced by stimulating the visual field at two areas of the same eccentricity and at the same temporal or nasal side but with one area superior to the horizontal raphe and the other area inferior to the raphe. The height from the calcarine sulcus was defined as the distance from an ECD to the crossing point of the calcarine sulcus with a line connecting the two symmetrical ECDs. The distance of ECDs from the
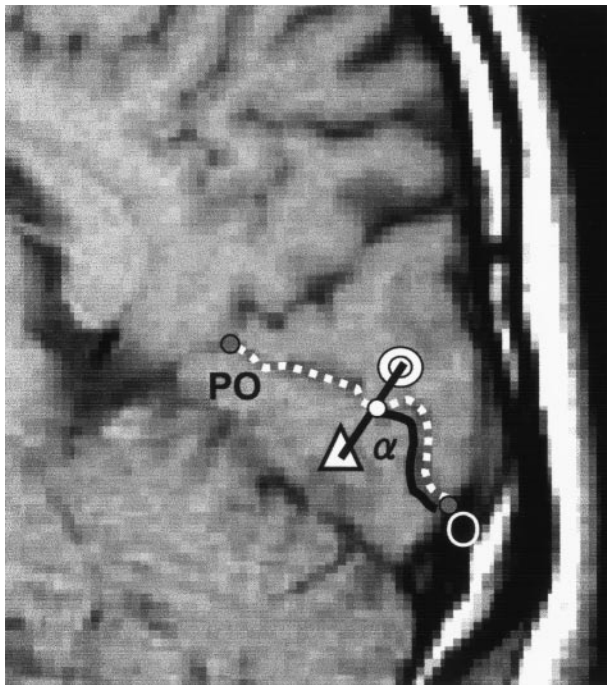
FIGURE 3. Height of ECDs from the calcarine sulcus. The MR image shows a sagittal view of the visual cortex. The crossing point (α) is the intersection of the *black straight line,* which connects the upper symmetrical ECD (*double circle*) and lower symmetrical ECD (*triangle*) with the calcarine sulcus. The height is the distance from the crossing point to an ECD. O, occipital pole; PO, parieto-occipital pole.

longitudinal fissure and the height of ECDs from the calcarine sulcus were measured digitally on MR images with an image-analysis program (NIH Image ver. 1.62; provided in the public domain by the National Institutes of Health, Bethesda, MD, and available at http://rsb.info.nih. gov/nih-image/). ECDs of all mVEF peaks from four quadrants of a stimulated visual field were plotted in the coordinates.

Difference in Depth of ECD from the Occipital Pole between mVEF-Estimated ECDs and Theoretical ECDs

The second coordinate plane corresponded to a sagittal section of an MR image. The abscissa shows depth of ECDs along the calcarine sulcus from the occipital pole to the crossing point of the calcarine sulcus with a line connecting the two symmetrical ECDs. The ordinate is along the previously mentioned height of ECDs from the calcarine sulcus (Fig. 2C). Because of interindividual variations in length and structure of the calcarine sulcus, standardization of the height and depth was determined with the total length of the calcarine sulcus as a reference. With this standardization, after the total length of the calcarine sulcus was measured on a sagittal MR image, a percentage ratio of the depths of ECDs to the total length of the calcarine sulcus was plotted on the abscissa axis. Units of the ordinate axis—namely, the upper-to-lower axis—were converted similarly to the ratio of the height of an ECD to the total length of the calcarine sulcus. The difference was examined between the depth of an mVEF-produced ECD and the theoretical depth, the latter of which was calculated with the human linear cortical magnification factor as described in the following section.

Theoretical Depth of the Activated Visual Cortex

Theoretical depth of the center of the activated visual cortex was calculated with the human linear cortical magnification factor method.

Horton and Hoyt[21] calculated the linear magnification factor in macaque striate cortex and used the data to estimate the factor in the human cortex. According to their investigations, the human linear cortical magnification factor is shown by the equation

$$M = 17.3/(E + 0.75)$$

where E is eccentricity in degrees.

Within the human visual striate cortex, the longer axis length, which is a prerequisite of this expression, is 80 mm. Therefore, the total length of the calcarine sulcus is 70 mm. This takes into account a 10-mm lateral convexity around the occipital pole. The eccentricity X corresponding to the lateral convexity around the occipital pole is calculated from the integral equation

$$10 = \int_0^x \frac{17.3}{E + 0.75} dE$$

which yields $X = 0.59$.

We did not stimulate regions less than $0.6°$ in radius from the center of the visual field, to avoid activating the lateral convexity around the occipital pole in which neural activity was the only radial component. The visual cortex was activated only in the interhemisphere in this experiment. At stimulation of the visual field from $0.59°$ to $10°$ of the radius, the theoretical depth (I) of the activated center from the occipital pole is

$$I = \int_{0.6}^{10} \frac{17.3}{E + 0.75} dE \times \frac{1}{2} \times \frac{1}{70} \times 100$$

which yields $I = 25.6\%$.

Source Localization of the Visual Cortex at Each Peak of the mVEFs

To increase the accuracy of the estimation, we examined only mVEFs with three peaks, each of which showed more than 95% GOF in both experiments, which were repeated twice. The position of ECDs, which were estimated from these highly reliable mVEFs, was examined to determine whether the ECDs were in V1 or other
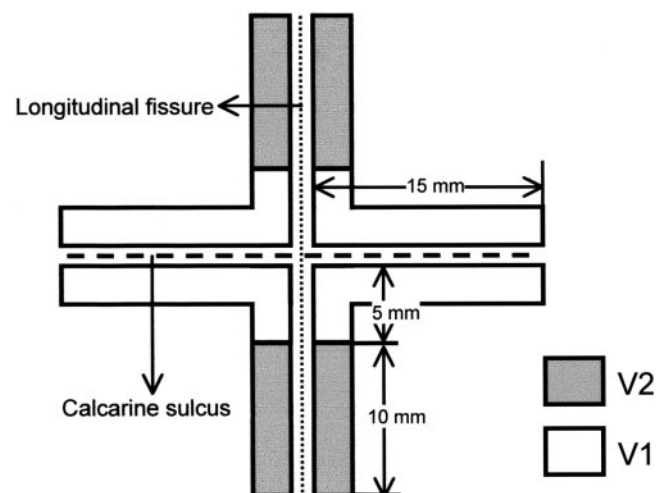

FIGURE 4. A simplified schema of the cerebral visual cortex. The calcarine sulcus plane is hypothesized to be a flat plane and to be at a right angle to the cerebral longitudinal fissure plane.
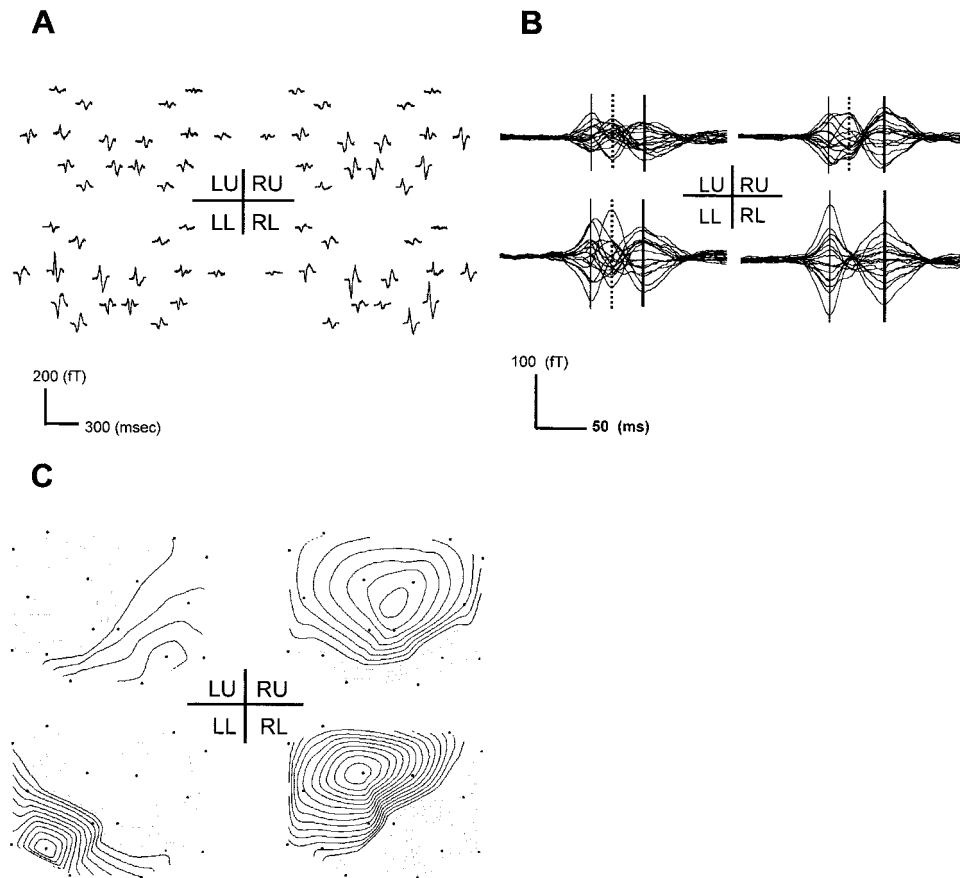
FIGURE 5. Magnetic responses derived from subject 1. (A) Superimposed traces of the first and second sets of 16 second-order responses calculated from magnetic fields from 16 sensors over the occipital head and corresponding to stimuli of four quadrants of two experiments are plotted. Amplitude, waveform, and response show good agreements. (B) mVEFs for stimuli of the four quadrant fields. All waveforms of the first slice of the second-order kernel calculated from magnetic fields recorded with 16 MEG channels over the occipital region were sorted and stacked together by stimulation quadrant. RU, right upper quadrant; LU, left upper quadrant; LL, left lower quadrant; RL, right lower quadrant. In subject 1, RU, LU, and LL showed three peaks, and RL showed two peaks at the same time, designated first peak (*thin, straight line*), middle peak (*dashed line*), and last peak (*bold line*). The waveforms of 84 of 112 (14 people × 4 sections × 2) responses had three peaks, and the waveforms of 28 had two peaks. (C) N75m isofield maps corresponding to each of the stimulated quadrants. *Black lines*: source of magnetic field; *gray lines*: the sink parameter.

regions, such as V2 or V3. The depth of ECDs from the occipital pole at each peak in the mVEFs was measured again along the direction of the calcarine sulcus in the coordinate plane that was comparable to the sagittal view of the MR image. The positions of the ECDs were examined again in the previously mentioned coordinate plane, which was similar to a coronal section of the MR image. The average of the abscissa and the average of the ordinate were obtained in ECDs at each mVEF peak. In this study, ECDs at three peaks in the mVEFs appeared 25% to 27% of the total length of the calcarine sulcus away from the occipital pole, as shown in previous studies. At a depth of approximately 26%, previous anatomic and functional MR imaging (f-MR imaging) studies[37–41] have shown that V1 extends along the calcarine sulcus 15 mm away from the longitudinal fissure and along the longitudinal fissure 5 mm from the calcarine sulcus, when viewed in the coronal plane. f-MR imaging has also shown that both V2 and V3 extend over 10 mm along the longitudinal fissure.[38,40] Using the data from these reports, we hypothesized a schema of V1, V2, and V3 in the coordinates of the coronal view (Fig. 4), and 95% confidence intervals of coordinates of ECDs were compared with coordinates of V1 in the schema.

Statistical Analysis

Statistical evaluation of the peak latency was performed with the two-way analysis of variance (ANOVA).

RESULTS

Peaks

One hundred twelve response waves (14 subjects × 4 stimulus fields × 2) were obtained. The waves were stable, and reproducibility was confirmed (Fig. 5A). Of the 112 waves, 84 (75%) had three peaks, and 28 (25%) had two peaks. The time series of waves, which were obtained from 16 channels at the same quadrant of visual fields, were overlaid (Fig. 5B). Latencies of the first peak were 79.4 ± 3 .1 ms in two-peak waves and 78.9 ± 3.8 ms in three-peak waves. Latencies of the last peak were 135.7 ± 6.9 ms in two-peak waves and 135.0 ± 7.0 ms in three-peak waves. When assessed with ANOVA, the difference in the first peak latency between three-peak waves and two-
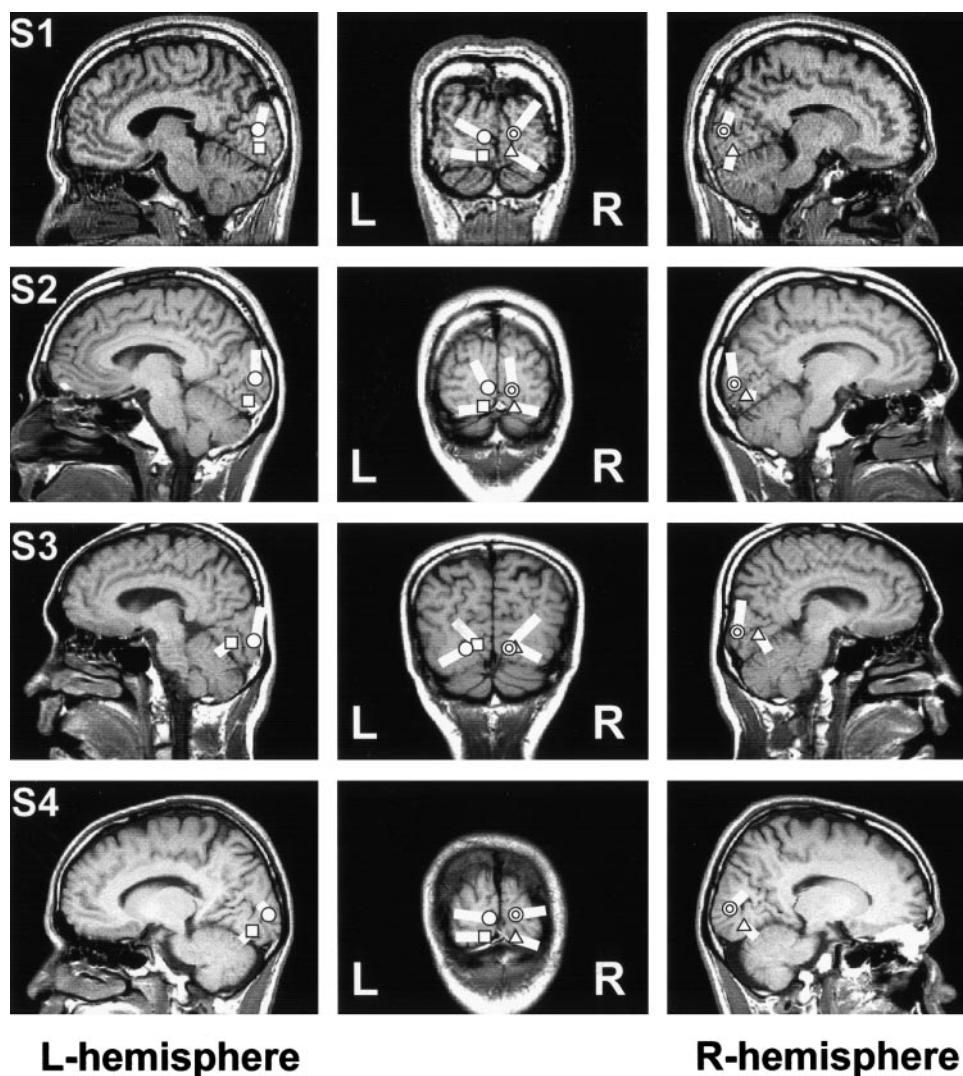
FIGURE 6.   Representative ECDs to each stimulated quadrant of the N75m peak in four subjects (S1–S4). ECDs were superimposed on right (R) sagittal, left (L) sagittal, and coronal sections of the MR images. From *left* to *right*: right hemisphere sagittal view, coronal view, and left hemisphere sagittal view are shown. Indicated are ECDs to right upper (*squares*), left upper (*triangles*), left lower (*double circles*), and right lower (*single circle*) quadrants. *White bars*: directions and intensities of ECDs.

peak waves was insignificant ($P = 0.584$). In addition, no significant difference was found in the latency of the last peak between three-peak waves and two-peak waves ($P = 0.742$). Therefore, the first and second peaks of the two-peak waves corresponded to the first and last peaks of the three-peak waves. In the present study, the waves with three peaks and those with two were considered similar. Thus, mean total latencies of waves were 79.3 ± 3.6 ms for the first peak, 99.9 ± 6.2 ms for the center peak, and 135.6 ± 7.ms for the last peak. Because of similarity to the peak latencies of the conventional VEP,[42] the first peak of the two-peak and three-peak mVEF waves was defined as N75m, the second peak of the three-peak waves was defined as P100m, and the last peak of the two-peak and three-peak waves were defined as N145m. N75m and N145m occurred in 100% of responses and P100m in 75%. Isocontour maps of all peaks suggested four single dipoles in the occipital area, with each map corresponding to one of the four quadrants of the stimulated visual fields. The maps of N75m only are shown in Figure 5C.

Dipole Estimation and MR Imaging at Peaks of All mVEFs

In all subjects, GOF of ECDs at the peaks was $97.0\% \pm 3.1\%$ for the N75m peak, $97.2\% \pm 3.2\%$ for the P100m, and $97.7\% \pm 2.4\%$ for the N145m. When the ECDs were overlaid on MR images, the anatomic relation between the stimulated visual field quadrant and the ECD location was consistent with the cruciform model at any mVEF peak in all subjects. That is, an ECD in response to the right or left visual field stimulation appeared in the left or right cerebral hemisphere, respectively. An ECD in response to the upper or lower visual field stimulation appeared in the visual cortex region at the lower or upper side of the calcarine sulcus, respectively (Fig. 6). When ECDs from the four quadrants of the visual field were plotted in the coordinates corresponding to the coronal view of MR images, all plots fit the expectations of the cruciform model at the all mVEF peaks (Fig. 7).
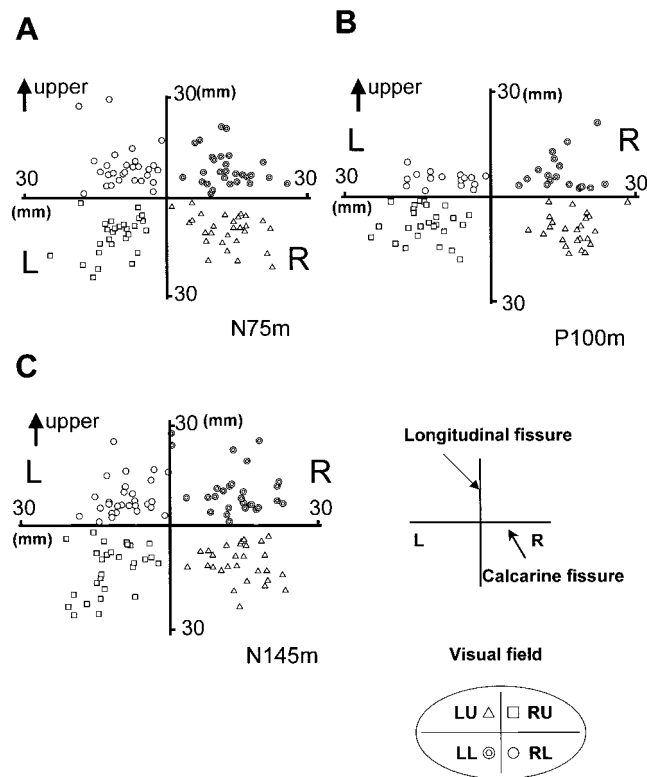
FIGURE 7. Coronal view of summarized ECD positions at individual stimulation of each visual field quadrant. At each peak time of mVEFs (**A**) N75m, (**B**) P100m, (**C**) N145m, positions of ECDs in the visual cortex of all subjects were plotted along the longitudinal fissure for the ordinate axis and the calcarine fissure for transverse axis. In this coordinate plane, the left hemisphere and upper side of the calcarine fissure are assumed to be positive. L, left; R, right; RU, right upper; RL, right lower; LU, left upper; LL, left lower.

Difference in Depth of ECD from the Occipital Pole between mVEF-Estimated ECDs and Theoretical ECDs

The depth of ECDs along the calcarine sulcus in the left hemisphere was 24.8% ± 8.2% for the N75m peak, 27.3% ± 3% for the P100m, and 27.3% ± 7.6% for the N145m. In the right hemisphere, the depth was 26.1% ± 7.6% for the N75m peak, 21.4% ± 4.5% for the P100m, and 26.1% ± 8.2% for the N145m (Fig. 8). All percentages at all peaks from all subjects were similar to the theoretical value (25.6%), which was calculated from the human linear cortical magnification factor (Fig. 9).

Source Localization in the Visual Cortex at Each Peak in the mVEF

The number of mVEFs with three peaks in twice-repeated experiments and with all peaks of more than 95% GOF was 44, and the GOFs of the peaks were 98.0% ± 1.2% at the N75m peak, 98.1% ± 1.1% at the P100m, and 98.0% ± 1.3% at the N145m. The ECDs were determined in 19 cerebral hemispheres of 10 subjects. The depths of the ECDs along the calcarine sulcus from the occipital pole were 24.6% ± 7.4% (actual length, 11.3 ± 3.7 mm) at the N75m peak, 27.1% ± 10.0% (14.2 ± 5.0 mm) at the P100m, and 25.5% ± 7.6% (12.1 ± 3.8 mm) at the N145m. The coordinates of the ECDs in the coronal view were 9.7 ± 4.7 mm and 3.9 ± 2.6 mm at the N75m peak, 13.0 ± 5.5 mm and 3.6 ± 2.6 mm at the P100m, and 10.9 ± 5.5 mm and 4.2 ± 3.0 mm at the N145m,

in order of the calcarine fissure side and the longitudinal fissure side. Figure 10A shows three ECDs superimposed on a coronal MR image of subject 6. The 95% confidence index of the mean coordinates of the ECDs were 9.7 ± 1.4mm and 3.9 ± 0.8 mm at the N75m peak, 13.0 ± 1.6 mm and 3.6 ± 0.8 mm at the P100m, and 10.9 ± 1.6 mm and 4.2 ± 0.9 mm at the N145m. The regions of these ECDs were within the previously reported regions of V1 (Fig. 10B).

DISCUSSION

The cerebral visual cortex showed interindividual anatomic differences, differences between the two cerebral hemispheres even in the same person, and asymmetrical structure above and below the calcarine sulcus.[37] These anatomic differences and the nature of the MEG, the latter of which can detect only a current that is tangential to the skull,[43] probably are the reasons for the relatively low frequency of appearance of P100m, which occurred at a rate of 75%, whereas the rate was 100% for the N75m and N145m peaks. Thus, further studies with a smaller size of stimulation in the mVEF or in combination with EEG, the latter of which can detect all directions of neural activity, are necessary to improve the decreased frequency of the P100m peak. Nevertheless, because the average GOF of the ECDs was acquired at approximately 97%, it is likely that reliable responses were obtained from all the sampling points. In addition to the decreased frequency of the P100m peak, the anatomic variation of the visual cortex may produce some difference in the coordinates of the ECDs. Although precise analysis of the ECD coordinates may need functional MR imaging or a flattened-cortex technique,[40] along with mVEF, we think that the number of the examined cerebral hemispheres in our study is large enough to allow us compare our results with those of previous reports on functional structure of the visual cortex. The ECD locations obtained with the m-sequence technique agreed well with both the cruciform model and the human linear cortical magnification factor model, both of which show the functional structure of the visual cortex. Thus, our results suggest that mVEF can be a reliable examination of visual cortex function and is a better functional test for estimation of ECDs in the visual cortex than mVEP is.

In our study, the estimated ECDs at each peak on mVEFs were shown within the V1 region. We think that it is important that the ECDs extended more than 9 mm from the cerebral fissure into the cerebral hemisphere. If only an extrastriate region, which is limited to a region of 2.5 mm width from the cerebral fissure and extending along the cerebral fissure,[44,45] is activated, the ECDs would not be seen to extend into the hemisphere for so long a distance (9 mm). Therefore, our results strongly suggest that ECDs at all peaks of mVEFs are in V1. Many factors contributed to our results. First, the large number of sensors is important. In a VEP study, when mVEP is measured by a single sensor, difficulty in obtaining a uniform response from all stimulus parts has been reported.[25,29,31] With use of the multifocal stimulation technique, the activated area is smaller than that activated by conventional full-field pattern VEP. Consequently, directions of each neural response corresponding to the multifocal activated visual cortex vary so that multiple sensors, which are matched for every direction, are necessary. In an mVEP study, two or five sensors are used instead of a single sensor, but there is disagreement about the appropriate positions of those sensors on the scalp.[31] Although an increase in the number of sensors solves the problem of positioning of electrodes,[26,46] an electrical shunt between closely positioned electrodes and variation in resistance between electrodes can increase, and operational difficulty in obtaining a reliable evoked response becomes considerable.
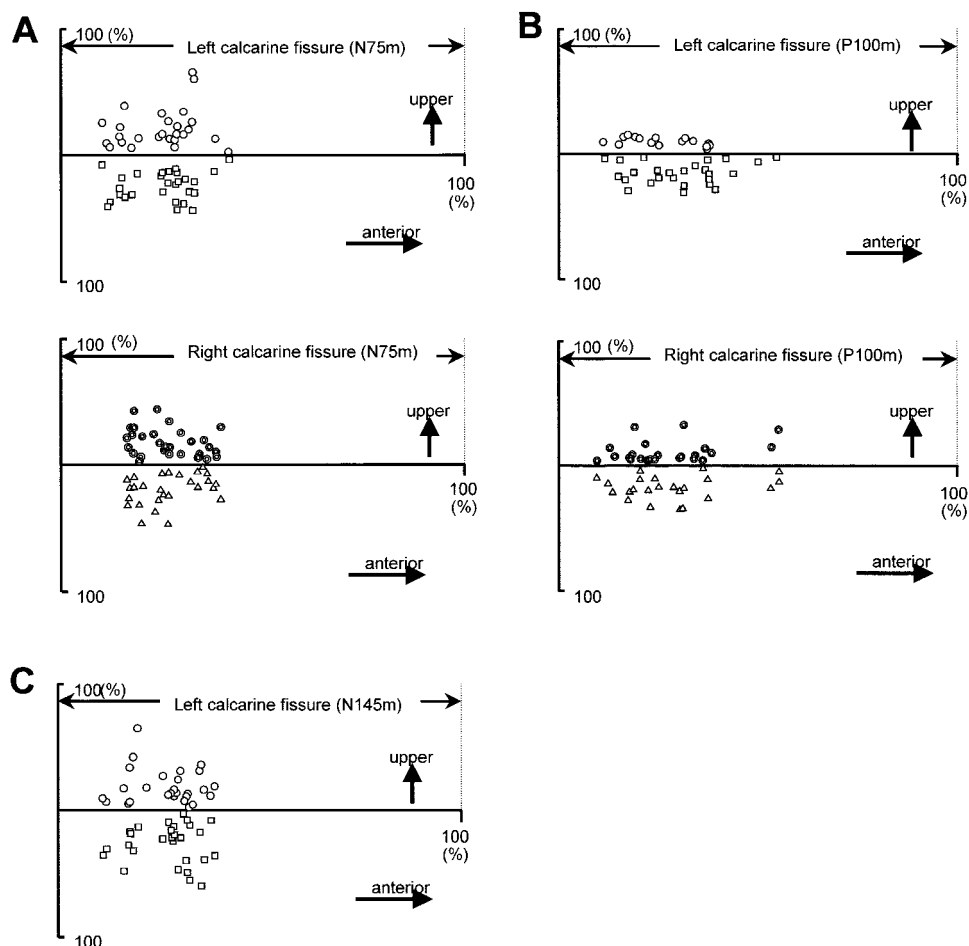
FIGURE 8. The percentage depth of ECDs from the occipital pole expressed as the ratio of ECD length to the total length of the calcarine sulcus. Responses of all subjects at each peak time are plotted: **(A)** N75m, **(B)** P100m, **(C)** N145m. The caudal point of the calcarine sulcus is defined as the zero point, and the upper side of the calcarine sulcus is assumed to be positive. To unite units of the axis, coordinates of the upper–lower axis have been converted to a ratio in relation to the calcarine sulcus.

Thus, MEG, which needs no sensor bonded to the scalp, is suitable for the m-sequence technique. With the m-sequence technique, multifocal, simultaneous stimulation can accurately

FIGURE 9. Mean ± SEM of the depth of the ECD from the occipital pole in each hemisphere at each peak time. *Dashed line:* theoretical depth of center of the area activated by simulation across 0.6° to 10° from center of the visual field (25.6%) as calculated with Horton's human linear cortical magnification factor.

delineate the active area of the visual cortex,[47] and the use of a high-frequency stimulator provides a better signal-to-noise ratio than the conventional method does. Therefore, a weak signal from a focal area of the cortex can be detected. In addition, the ability to accurately estimate an ECD with MEG is important. Another valuable benefit is that the data were collected in a relatively short time, less than 5 minutes. Shortcomings associated with conventional methods such as sleepiness, concentration loss, and unstable fixation can be avoided by this short recording period.

CONCLUSION

MEG, which no longer requires fixed sensors on the scalp, can detect simultaneous, multichannel responses produced with an m-sequence technique for visual field stimulation. The m-sequence technique adds three advantages to MEG: high temporal resolution of real-time recording of neural activity; excellent dipole estimation; and high signal-to-noise ratio over a short recording period. With this technique, the center of m-component activated areas was shown in V1 at all N75m, P100m, and N145m peak components of the mVEF.
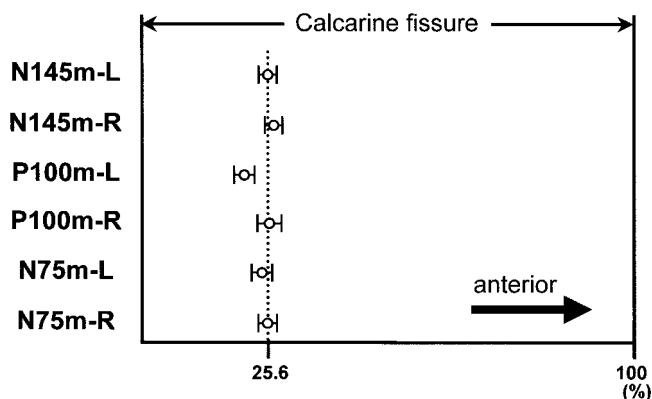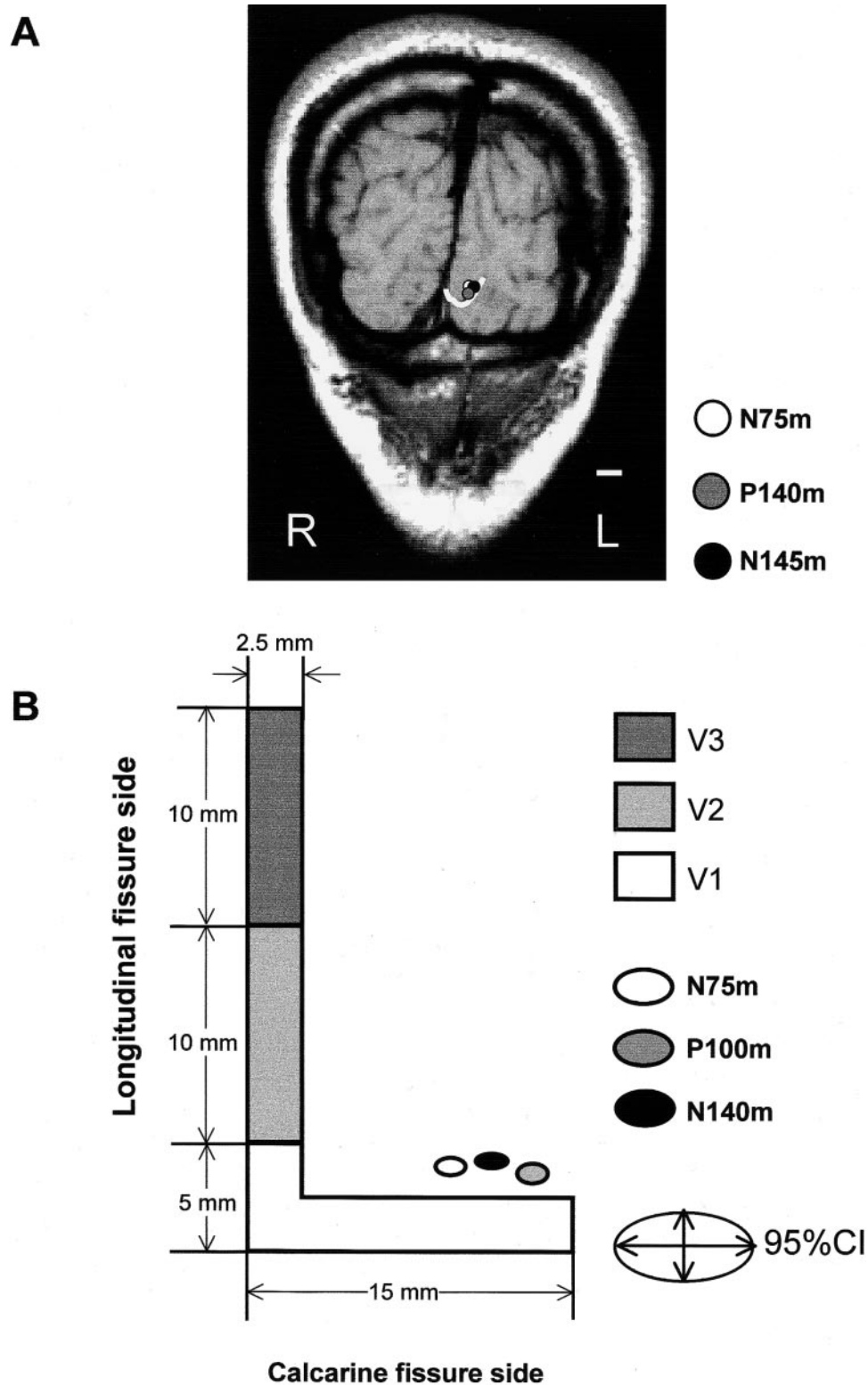
FIGURE 10. Location of ECDs of three components, N75m, P100m, N145m, on a coronal view. (**A**) ECDs of three components superimposed on the coronal MR image of subject 6. *White line*: calcarine sulcus. Bar, 10 mm. (**B**) Relation of striate (V1) and extrastriate (V2, V3) cortex with ECDs of 95% confidence index at each peak of selected mVEFs. The coordinate plane is similar to a coronal section of the MR image, with the longitudinal fissure as the ordinate and the calcarine sulcus as the abscissa. The regions of three *ovals* shows estimated ECD regions with 95% confidence index.

References

1. Halliday AM. The visual evoked potential in healthy subjects. In: Halliday AM, ed. *Evoked Potentials in Clinical Testing*. Edinburgh: Churchill Livingstone; 1993:57–113.

2. Cohen D, Magnetoencephalography: evidence of magnetic fields produced by alpha-rhythm currents. *Science.* 1968;161:784–786.

3. Cohen D, Cuffin BN, Yunokuchi K, et al. MEG versus EEG localization test using implanted sources in the human brain. *Ann Neurol.* 1990;28:811–817.

4. Brenner D, Williamson SJ, Kaufman L. Visually evoked magnetic fields of the human brain. *Science.* 1975;190:480–482.

5. Brecelj J, Kakigi R, Koyama S, Hoshiyama M. Visual evoked magnetic responses to central and peripheral stimulation: simultaneous VEP recordings. *Brain Topogr.* 1998;10:227–237.

6. Shigeto H, Tobimatsu S, Yamamoto T, Kobayashi T, Kato M. Visual evoked cortical magnetic responses to checkerboard pattern reversal stimulation: a study on the neural generators of N75, P100 and N145. *J Neurol Sci.* 1998;156:186–194.

7. Aine CJ, Supek S, George JS, et al. Retinotopic organization of human visual cortex: departures from the classical model. *Cereb Cortex.* 1996;6:354–361.

8. Nakamura A, Kakigi R, Hoshiyama M, Koyama S, Kitamura Y, Shimojo M. Visual evoked cortical magnetic fields to pattern reversal stimulation. *Brain Res Cogn Brain Res.* 1997;6:9–22.

9. Nakamura M, Kakigi R, Okusa T, Hoshiyama M, Watanabe K. Effects of check size on pattern reversal visual evoked magnetic field and potential. *Brain Res.* 2000;872:77–86.

10. Parker DM, Salzen EA, Lishman JR. Visual-evoked responses elicited by the onset and offset of sinusoidal gratings: latency, waveform, and topographic characteristics. *Invest Ophthalmol Vis Sci.* 1982;22:675–680.

11. Jones R, Keck MJ. Visual evoked response as a function of grating spatial frequency. *Invest Ophthalmol Vis Sci.* 1978;17:652–659.

12. Ghilardi MF, Sartucci F, Brannan JR, et al. N70 and P100 can be independently affected in multiple sclerosis. *Electroencephalogr Clin Neurophysiol.* 1991;80:1–7.

13. Hashimoto T, Kashii S, Kikuchi M, Honda Y, Nagamine T, Shibasaki H. Temporal profile of visual evoked responses to pattern-reversal stimulation analyzed with a whole-head magnetometer. *Exp Brain Res.* 1999;125:375–382.

14. Noachtar S, Hashimoto T, Luders H. Pattern visual evoked potentials recorded from human occipital cortex with chronic subdural electrodes. *Electroencephalogr Clin Neurophysiol.* 1993;88:435–446.

15. Jeffreys DA, Axford JG. Source locations of pattern-specific components of human visual evoked potentials. I: component of striate cortical origin. *Exp Brain Res.* 1972;16:1–21.

16. Butler SR, Georgiou GA, Glass A, Hancox RJ, Hopper JM, Smith KR. Cortical generators of the CI component of the pattern-onset visual evoked potential. *Electroencephalogr Clin Neurophysiol.* 1987;68:256–267.

17. Maier J, Dagnelie G, Spekreijse H, van Dijk BW. Principal components analysis for source localization of VEPs in man. *Vision Res.* 1987;27:165–177.

18. Ossenblok P, Spekreijse H. The extrastriate generators of the EP to checkerboard onset: a source localization approach. *Electroencephalogr Clin Neurophysiol.* 1991;80:181–193.

19. Jeffreys DA, Axford JG. Source locations of pattern-specific components of human visual evoked potentials. II: component of extrastriate cortical origin. *Exp Brain Res.* 1972;16:22–40.

20. Holmes G. The organization of the visual cortex in man. *Proc R Soc Lond B Biol Sci.* 1945;132;348–361.

21. Horton JC, Hoyt WF. The representation of the visual field in human striate cortex: a revision of the classic Holmes map. *Arch Ophthalmol.* 1991;109:816–824.

22. Dobelle WH, Turkel J, Henderson DC, Evans JR. Mapping the representation of the visual field by electrical stimulation of human visual cortex. *Am J Ophthalmol.* 1979;88:727–735.

23. Fox PT, Miezin FM, Allman JM, Van Essen DC, Raichle ME. Retinotopic organization of human visual cortex mapped with positron-emission topography. *J Neurosci.* 1987;7:913–922.

24. Sutter EE. Deterministic approach to nonlinear systems analysis. In: Printer RB, Nabet B, eds. *Nonlinear Vision.* Boca Roton, FL: CRC Press; 1992:171–220.

25. Baseler HA, Sutter EE, Klein SA, Carney T. The topography of visual evoked response properties across the visual field. *Electroencephalogr Clin Neurophysiol.* 1994;90:65–81.

26. Slotnick SD, Klein SA, Carney T, Sutter E, Dastmalchi S. Using multi-stimulus VEP source localization to obtain a retinotopic map of human primary visual cortex. *Clin Neurophysiol.* 1999;110:1793–1800.

27. Baseler HA, Sutter EE. M and P components of the VEP and their visual field distribution. *Vision Res.* 1997;37:675–690.

28. Klistorner A, Crewther DP, Crewther SG. Temporal analysis of the VEP: evidence for separable magnocellular and parvocellular contributions. *Aust NZ J Ophthalmol.* 1996;24:32–34.

29. Klistorner AI, Graham SL, Grigg JR, Billson FA. Multifocal topographic visual evoked potential: improving objective detection of local visual field defects. *Invest Ophthalmol Vis Sci.* 1998;39:937–950.

30. Klistorner A, Graham SL. Objective perimetry in glaucoma. *Ophthalmology.* 2000;107:2283–2299.

31. Hood DC, Zhang X, Greenstein VC, et al. An interocular comparison of the multifocal VEP: a possible technique for detecting local damage to the optic nerve. *Invest Ophthalmol Vis Sci.* 2000;41:1580–1587.

32. Hood DC, Zhang X. Multifocal ERG and VEP responses and visual fields: comparing disease-related changes. *Doc Ophthalmol.* 2000;100:115–137.

33. Hood DC, Odel JG, Zhang X. Tracking the recovery of local optic nerve function after optic neuritis: a multifocal VEP study. *Invest Ophthalmol Vis Sci.* 2000;41:4032–4038.

34. Higuchi M, Shimogawara M, Haruta Y, et al. System integration and trade-off of SQUID system for biomagnetic applications. *Appl Superconduct.* 1998;5:441–449.

35. Sarvas J. Basic mathematical and electromagnetic concepts of the biomagnetic inverse problem. *Phys Med Biol.* 1987;32:11–22.

36. Kaukoranta E, Hamalainen M, Sarvas J, Hari R. Mixed and sensory nerve stimulations activate different cytoarchitectonic area in the human primary somatosensory cortex SI: neuromagnetic recordings and statistical considerations. *Exp Brain Res.* 1986;63:60–66.

37. Stensaas SS, Eddington DK, Dobelle WH. The topography and variability of the primary visual cortex in man. *J Neurosurg.* 1974;40:747–755.

38. Wandell BA. Computational neuroimaging of human visual cortex. *Annu Rev Neurosci.* 1999;22:145–173.

39. Engel SA, Glover GH, Wandell BA. Retinotopic organization in human visual cortex and the spatial precision of functional MRI. *Cereb Cortex.* 1997;7:181–192.

40. Sereno MI, Dale AM, Reppas JB, et al. Borders of multiple visual areas in humans revealed by functional magnetic resonance imaging. *Science.* 1995;12:268:889–893.

41. DeYoe EA, Carman GJ, Bandettini P, et al. Mapping striate and extrastriate visual areas in human cerebral cortex. *Proc Natl Acad Sci USA.* 1996;93:2382–2386.

42. American Electroencephalographic Society. Guidelines for clinical evoked potential studies. *J Clin Neurophysiol.* 1984;1:3–53.

43. Sutherling WW, Cuffin BN, Hari R, et al. Assessment: magnetoencephalography (MEG). Report of the Therapeutics and Technology Assessment Subcommittee of the American Academy of Neurology. *Neurology.* 1992;41:1–4.

44. Zilles K. In: Paxinos G, ed. *The Human Nervous System.* San Diego, CA: Academic Press; 1990:757–802.

45. Fischl B, Dale AM. Measuring the thickness of the human cerebral cortex from magnetic resonance images. *Proc Natl Acad Sci USA.* 2000;97:11050–11055.

46. Jedynak A, Skrandies W. Functional perimetry combined with topographical VEP analysis. *Int J Neurosci.* 1998;93:117–132.

47. Usui S, Nagasaka E. Spatial distribution of local flash electroretinogram by multi-input stimulation. *Doc Ophthalmol.* 1994;88:57–63.